TWO-VALENCE-PARTICLE NUCLEI IN THE ^{132}Sn AND ^{208}Pb REGIONS*

A. Covello[a,b], L. Coraggio[b], A. Gargano[b], N. Itaco[a,b]

[a]Dipartimento di Scienze Fisiche, Università di Napoli Federico II
Complesso Universitario di Monte S. Angelo
Via Cintia, I-80126 Napoli, Italy
[b]Istituto Nazionale di Fisica Nucleare
Complesso Universitario di Monte S. Angelo
Via Cintia, I-80126 Napoli, Italy

(Received November 10, 2008)

We report on a shell-model study of nuclei with two valence nucleons in the ^{132}Sn and ^{208}Pb regions, focusing attention on the similarity between the spectroscopy of these two regions. In our study we make use of realistic effective interactions derived from the CD-Bonn nucleon–nucleon potential renormalized by use of the $V_{\mathrm{low}-k}$ approach. We show that the behavior of the proton–proton, neutron–neutron and proton–neutron multiplets in ^{134}Te, ^{134}Sn and ^{134}Sb, respectively, is quite similar to that of the analogous multiplets in the counterpart nuclei in the ^{208}Pb region, ^{210}Po, ^{210}Pb and ^{210}Bi.

PACS numbers: 21.60.Cs, 21.30.Fe, 27.60.+j, 27.80.+w

1. Introduction

The study of nuclei around double shell closures plays a key role in understanding the properties of the effective interaction between valence nucleons. In this context, of special interest are nuclei in the close vicinity to ^{132}Sn and ^{208}Pb, which show strong shell closures for both protons and neutrons.

Experimentally, while nuclei neighboring ^{208}Pb have long been the subject of experimental studies, this is not the case for the ^{132}Sn neighbors, which lie well away from the valley of stability. In recent years, however, substantial progress has been made to access the regions of shell closures off

* Presented at the Zakopane Conference on Nuclear Physics, September 1–7, 2008, Zakopane, Poland.

stability, which has made it possible to gain more information on neutron-rich nuclei around ^{132}Sn. The new data which are becoming available for this region allow one to investigate more quantitatively the resemblance between the spectroscopy of this region and that of nuclei around ^{208}Pb, which has been pointed out in several recent papers [1–3].

With the above motivation, we have performed shell-model calculations for the two-valence-particle neighbors of ^{132}Sn, ^{134}Te, ^{134}Sn and ^{134}Sb, as well as for their counterparts in the ^{208}Pb region, ^{210}Po, ^{210}Pb and ^{210}Bi. In this paper, we shall focus attention on the behavior of the lowest particle-particle multiplets in these three counterpart pairs.

In our calculations we have employed realistic effective interactions derived from the CD-Bonn nucleon–nucleon (NN) potential [4]. The short-range repulsion of the latter is renormalized by constructing a smooth low-momentum potential, $V_{\mathrm{low}-k}$, that is used directly as input for the calculation of the effective interaction.

The outline of the paper is as follows. In Sec. 2 we give a brief description of the theoretical framework in which our calculations have been performed. In Sec. 3 we present and discuss the results of our calculations. Some concluding remarks are given in Sec. 4.

2. Outline of theoretical framework

The shell-model effective interaction V_{eff} is defined, as usual, in the following way. In principle, one should solve a nuclear many-body Schrödinger equation of the form

$$H\,\Psi_i = E_i\,\Psi_i\,, \tag{1}$$

with $H = T + V_{NN}$, where T denotes the kinetic energy. This full-space many-body problem is reduced to a smaller model-space problem of the form

$$P H_{\mathrm{eff}} P\,\Psi_i = P(H_0 + V_{\mathrm{eff}})P\,\Psi_i = E_i P\,\Psi_i\,. \tag{2}$$

Here $H_0 = T + U$ is the unperturbed Hamiltonian, U being an auxiliary potential introduced to define a convenient single-particle basis, and P denotes the projection operator onto the chosen model space.

As pointed out in the Introduction, we "smooth out" the strong repulsive core contained in the bare NN potential V_{NN} by constructing a low-momentum potential $V_{\mathrm{low}-k}$. This is achieved by integrating out the high-momentum modes of V_{NN} down to a cutoff momentum Λ. This integration is carried out with the requirement that the deuteron binding energy and phase shifts of V_{NN} up to Λ are preserved by $V_{\mathrm{low}-k}$. A detailed description of the derivation of $V_{\mathrm{low}-k}$ from V_{NN} as well as a discussion of its main features can be found in Refs. [5, 6].

Once the $V_{\mathrm{low}-k}$ is obtained, we use it as input interaction for the calculation of the matrix elements of the shell-model effective interaction. The latter is derived by employing a folded-diagram method, which was previously applied to many nuclei using G-matrix interactions [7]. Since $V_{\mathrm{low}-k}$ is already a smooth potential, it is no longer necessary to calculate the G matrix. We therefore derive V_{eff} following the same procedure as described, for instance, in Refs. [8, 9], except that the G matrix used there is replaced by $V_{\mathrm{low}-k}$. More precisely, we first calculate the so-called $\hat{Q}$-box [10] including diagrams up to second order in $V_{\mathrm{low}-k}$. The shell-model effective interaction is then obtained by summing up the $\hat{Q}$-box folded diagram series using the Lee-Suzuki iteration method [11].

3. Calculations and results

In our calculations for ^{134}Te, ^{134}Sn and ^{134}Sb we assume that the valence protons occupy the five levels $0g_{7/2}$, $1d_{5/2}$, $1d_{3/2}$, $2s_{1/2}$, and $0h_{11/2}$ of the 50-82 shell, while for the neutrons the model space includes the six levels $0h_{9/2}$, $1f_{7/2}$, $1f_{5/2}$, $2p_{3/2}$, $2p_{1/2}$, and $0i_{13/2}$ of the 82–126 shell. Similarly, for ^{210}Po, ^{210}Pb and ^{210}Bi we take as model space for the valence protons the six levels of the 82–126 shell and let the valence neutrons occupy the seven levels $1g_{9/2}$, $0i_{11/2}$, $0j_{15/2}$, $2d_{5/2}$, $3s_{1/2}$, $1g_{7/2}$, and $2d_{3/2}$ of the 126–184 shell.

As regards the choice of the single-proton and single-neutron energies, we have proceeded as follows. For the ^{132}Sn region nuclei, we have taken them from the experimental spectra of ^{133}Sb and ^{133}Sn, with the exception of the proton $s_{1/2}$ and the neutron $i_{13/2}$ levels, which are still missing. The values of $\epsilon_{s_{1/2}}$ and $\epsilon_{i_{13/2}}$ have been taken from Refs. [12] and [13], respectively, where it is discussed how they are determined. In the same way, for the nuclei around ^{208}Pb, we have made use of the experimental spectra of ^{209}Bi and ^{209}Pb. The adopted values of the single-particle energies are reported in Refs. [14] and [15] for the ^{132}Sn and ^{208}Pb regions, respectively.

As outlined in Sec. 2, in our shell-model calculations we have employed effective interactions derived from the CD-Bonn NN potential renormalized through the $V_{\mathrm{low}-k}$ procedure. As in our previous studies [14–18], the cutoff momentum Λ is given the value 2.2 fm^{-1}. The computation of the diagrams included in the $\hat{Q}$ box is performed within the harmonic-oscillator basis using intermediate states composed of all possible hole states and particle states restricted to the five proton and neutron shells above the Fermi surface. The oscillator parameter is 7.88 MeV for the $A = 132$ region and 6.88 MeV for the $A = 208$ region, as obtained from the expression $\hbar\omega = 45A^{-1/3} - 25A^{-2/3}$.

Let us now come to the results of our calculations, which have been performed by using the NushellX shell-model code [19].

In Table I, II and III, we report the experimental [20, 21] and calculated excitation energies of the members of the proton–proton, neutron–neutron, and proton–neutron multiplets arising from the configurations $(\pi g_{7/2})^2$ and $(\pi h_{9/2})^2$ in ^{134}Te and ^{210}Po, $(\nu f_{7/2})^2$ and $(\nu g_{9/2})^2$ in ^{134}Sn and ^{210}Pb, $\pi g_{7/2}\nu f_{7/2}$ and $\pi h_{9/2}\nu g_{9/2}$ in ^{134}Sb and ^{210}Bi, respectively. In these tables the percentage of the corresponding configurations is also shown.

TABLE I

Experimental and calculated energies of the members of the proton–proton multiplet $(\pi g_{7/2})^2$ in ^{134}Te and $(\pi h_{9/2})^2$ in ^{210}Po. The percentage of the corresponding configuration is reported for each state.

	^{134}Te			^{210}Po		
J^π	Exp.	Calc.	%	Exp.	Calc.	%
0^+	0.0	0.0	80	0.0	0.0	77
2^+	1.279	1.332	96	1.181	1.222	97
4^+	1.576	1.605	98	1.427	1.458	99
6^+	1.691	1.749	98	1.473	1.538	99
8^+				1.557	1.622	99

TABLE II

Experimental and calculated energies of the members of the neutron–neutron multiplet $(\nu f_{7/2})^2$ in ^{134}Sn and $(\nu g_{9/2})^2$ in ^{210}Pb. The percentage of the corresponding configuration is reported for each state.

	^{134}Sn			^{210}Pb		
J^π	Exp.	Calc.	%	Exp.	Calc.	%
0^+	0.0	0.0	81	0.0	0.0	71
2^+	0.725	0.734	86	0.800	0.709	95
4^+	1.073	1.016	95	1.098	0.923	99
6^+	1.247	1.125	98	1.195	1.009	99
8^+				1.278	1.060	99

We see that the agreement between experiment and theory is very good for all the six nuclei considered, the discrepancies being well below 100 keV for the large majority of states. Note that the wave functions of the members of the various multiplets are characterized by very little configuration mixing, the percentage of the leading component ranging from 94% to 100% for most of the states.

To give more emphasis to the striking resemblance between the spectroscopy of the ^{132}Sn and ^{208}Pb regions, in Figs. 1–3 we compare the behavior of the calculated multiplets in the three counterpart pairs, ^{134}Te and

TABLE III

Experimental and calculated energies of the members of the proton–neutron multiplet $\pi g_{7/2}\nu f_{7/2}$ in ^{134}Sb and $\pi h_{9/2}\nu g_{9/2}$ in ^{210}Bi. The percentage of the corresponding configuration is reported for each state.

	^{134}Sb			^{210}Bi		
J^π	Exp.	Calc.	%	Exp.	Calc.	%
0^-	0.0	0.0	95	0.047	0.026	97
1^-	0.013	0.052	94	0.0	0.0	91
2^-	0.331	0.385	88	0.320	0.344	96
3^-	0.383	0.419	94	0.348	0.359	97
4^-	0.555	0.621	94	0.503	0.522	98
5^-	0.442	0.494	94	0.439	0.456	98
6^-	0.617	0.727	94	0.550	0.585	98
7^-	0.279	0.407	100	0.433	0.464	98
8^-				0.583	0.628	97
9^-				0.271	0.361	100

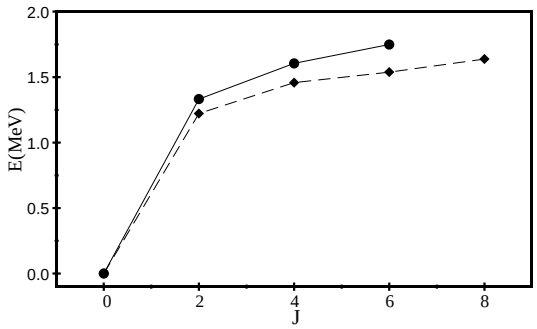

Fig. 1. Calculated proton–proton multiplets in ^{134}Te (circles) and ^{210}Po (diamonds).

^{210}Po, ^{134}Sn and ^{210}Pb, ^{134}Sb and ^{210}Bi. We see that in each of these figures the two curves show the same behavior, the one relative to the nucleus in the ^{208}Pb region being located slightly below that for the counterpart nucleus in the ^{132}Sn region. The only exception occurs in Fig. 3, where the 7^- state in ^{210}Bi lies above the corresponding one in ^{134}Sb.

Comparison of Figs. 1 and 2, which refer to the two-valence-proton and two-valence-neutron systems, respectively, gives direct evidence of the difference between proton–proton and neutron–neutron interactions. We note that both the two curves of Fig. 2 are located in an energy interval significantly smaller than that pertaining to the curves of Fig. 1, namely for the two-neutron case there is a smaller gap between the ground and excited

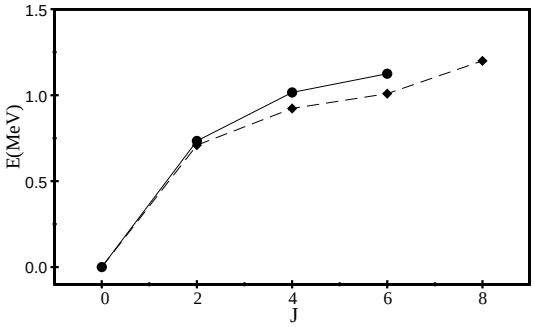

Fig. 2. Calculated neutron–neutron multiplets in ^{134}Sn (circles) and ^{210}Pb (diamonds).

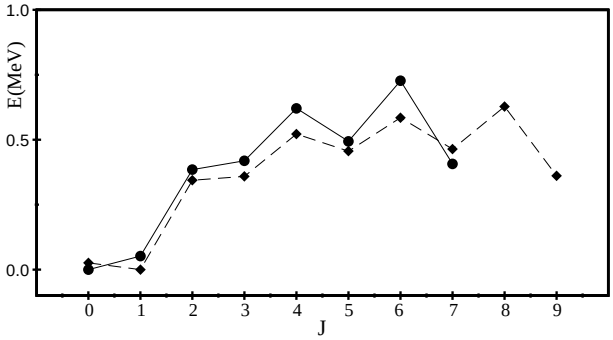

Fig. 3. Calculated proton–neutron multiplets in ^{134}Sb (circles) and ^{210}Bi (diamonds).

states. This is a manifestation of the weakening of the pairing force between neutrons beyond the $N = 82$ closed shell [22, 23]. As regards the proton–neutron interaction, from Fig. 3 we see that, while it is not so strong as that between identical particles, it produces a distinctive energy staggering between the odd and even spin members of the multiplet.

4. Summary and conclusions

We have presented here the results of a shell-model study of nuclei around doubly magic ^{132}Sb and ^{208}Pb, focusing attention on proton–proton, neutron–neutron and proton–neutron multiplets. We have compared the results obtained for the three far from stability nuclei ^{134}Te, ^{134}Sn and ^{134}Sb with those for ^{210}Po, ^{210}Pb and ^{210}Pb, which are their counterparts in the region of stable ^{208}Pb. In both cases, the two body effective interaction has been derived by means of a $\hat{Q}$-box folded-diagrams method from the

CD-Bonn NN potential, the short-range repulsion of the latter being renormalized by use of the low-momentum potential $V_{\mathrm{low}-k}$. It should be stressed that no adjustable parameter appears in our calculations.

Our results for all six nuclei are in very good agreement with the experimental data and account for the striking resemblance between the behavior of the multiplets in the ^{132}Sn and ^{208}Pb regions. This stimulates further studies to find out whether this resemblance extends beyond the two-valence-particle nuclei.

REFERENCES

[1] B. Fornal *et. al.*, *Phys. Rev.* **C63**, 024322 (2001).

[2] V.I. Isakov *et al.*, *Phys. At. Nucl.* **70**, 818 (2006).

[3] A. Korgul *et al.*, *Eur. Phys. J.* **A32**, 25 (2007).

[4] R. Machleidt, *Phys. Rev.* **C63**, 024001 (2001).

[5] S. Bogner *et. al.*, *Phys. Rev.* **C65**, 051301(R) (2002).

[6] A. Covello *et. al.*, *J. Phys.: Conference Series* **20**, 137 (2005).

[7] A. Covello *et. al.*, *Acta Phys. Pol. B* **32**, 871 (2001) and references therein.

[8] M.F. Jiang *et. al.*, *Phys. Rev.* **C46**, 910 (1992).

[9] A. Covello *et. al.*, *Prog. Part. Nucl. Phys.* **38**, 165 (1997).

[10] T.T.S. Kuo, E. Osnes, *Lecture Notes in Physics*, vol. 364, Springer-Verlag, Berlin 1990.

[11] K. Suzuki, S.Y. Lee, *Prog. Theor. Phys.* **64**, 2091 (1980).

[12] F. Andreozzi *et. al.*, *Phys. Rev.* **C56**, R16 (1997).

[13] L. Coraggio, A. Covello, A. Gargano, N. Itaco, *Phys. Rev.* **C65**, 051306 (2002).

[14] L. Coraggio, A. Covello, A. Gargano, N. Itaco, *Phys. Rev.* **C72**, 057302 (2005).

[15] L. Coraggio, A. Covello, A. Gargano, N. Itaco, *Phys. Rev.* **C76**, 061303 (2007).

[16] L. Coraggio, A. Covello, A. Gargano, N. Itaco, *Phys. Rev.* **C73**, 031302 (2006).

[17] A. Covello *et. al.*, *Eur. Phys. J. ST* **150**, 93 (2007).

[18] G.S. Simpson *et. al.*, *Phys. Rev.* **C76**, 041303(R) (2007).

[19] NushellX for Linux, produced by William D.M. Rae, Garsington, Oxford, 2007/08, `http://knollhouse.org.`

[20] Data extracted using the NNDC On-line Data Service from the ENSDF database, version of November 3, 2008.

[21] J. Shergur *et al.*, *Phys. Rev.* **C71**, 064321 (2005).

[22] J. Terasaki, J. Engel, W. Nazarewicz, M. Stoitsov, *Phys. Rev.* **C66**, 054313 (2002).

[23] N. Shimizu, T. Otsuka, T. Mizusaki, M. Honma, *Phys. Rev.* **C70**, 054313 (2004).